

A Critical Evaluation of Indentation Techniques for Measuring Fracture Toughness: II, Strength Method

P. CHANTIKUL, G. R. ANSTIS, B. R. LAWN,* and D. B. MARSHALL*.*

Department of Applied Physics, School of Physics, University of New South Wales, New South Wales 2033, Australia

An examination is made of the sharp-indentation technique of strength-test precracking for toughness evaluation. The experimental approach follows that proposed by other workers but the theoretical analysis contains one vital new feature; the residual-stress term discussed in Part I of this study is now introduced explicitly into the strength formulation. This modification overcomes a major systematic discrepancy evident in the previous models and at the same time, by virtue of attendant changes in the nature of the crack stability prior to attaining a failure configuration, eliminates the need for fractographic measurements. Other advantages are also apparent, notably an insensitivity to postindentation radial crack extension. The main disadvantage is that only one result is obtained per specimen. Indentation/strength data from ceramics listed in Part I confirm the essential features of the theory and provide a suitable calibration factor. The method has special application to those materials which do not necessarily produce a well-defined radial crack pattern, in which case an "effective" K_{Ic} appropriate to fracture properties at the flaw level is obtained.

I. Introduction

IN THIS paper an alternative adaptation of the indentation approach to toughness measurement is investigated. The central idea is that the radial crack system be used as a dominant flaw in a strength test piece. Then, in conjunction with an appropriate fracture mechanics analysis for cracks in tensile loading, standard strength formulas may be used to determine K_{Ic} . A form of this "controlled-flaw" approach has been used by others,¹⁻⁶ on a range of brittle materials, in which detailed measurement of the flaw dimensions is an essential step in the analysis (for a review see Ref. 7). However, two major disadvantages are apparent in such studies: (i) The subsurface flaw geometry is not always clearly delineated on the section faces of the fractured test piece (in which case the method would appear to hold no real advantage over that described in Part I¹); (ii) a systematic discrepancy exists between the toughness evaluated from the strength equation and that determined from more conventional fracture specimens (e.g. double cantilever, double torsion), with the former consistently lower by some 30 to 40%.²⁻⁴ While it has been duly recognized that the residual contact field associated with the radial crack system is the chief source of the discrepancy in this case,^{9,10} no serious attempt has been made to incorporate a residual stress intensity factor term into the strength/toughness formulation. Rather, special experimental stratagems aimed at nullifying the residual stresses (e.g. annealing, physical removal of central deformation zone) have been explored.⁹ Apart from greatly complicating the test procedure, this particular approach runs the risk of altering the character of the indentation flaw⁷; analysis of data then requires careful attention to be paid to the entire postindentation history of the crack system.

Here a modified form of the controlled-flaw concept is proposed. Using the results for the elastic/plastic indentation fracture analysis summarized in Part I, a residual-stress term is introduced explicitly into the strength equations.¹¹⁻¹³ In this way the systematic discrepancy referred to above is automatically removed, thus eliminating the need to resort to special postindentation treatments:

Moreover, by virtue of ensuing modifications to the conditions of crack stability prior to failure,¹² flaw size is eliminated as a test variable in favor of indentation load. The need for accurate crack measurements is thereby avoided, a distinct benefit in any form of fracture testing. Coupling this with a relative insensitivity to slow crack growth effects, the method offers certain advantages over that of Part I (at some expense, of course, in test-piece economy). Furthermore, departures from well-defined crack geometries due to microstructural or other complications do not pose quite the same limitations as they do in Part I: in such cases the test provides a measure of "effective" toughness which, although perhaps not representative of the toughness value obtained from macroscopic crack measurements in conventional fracture mechanics arrangements, may be expected to reflect more closely the behavior of microscopic flaws which control the strengths of real ceramics.

The experimental procedure adopted in the following study closely parallels that used in the previous direct crack measurement method,⁸ insofar as choice of materials for testing and the indentation system are concerned, to allow for useful comparison between the alternative approaches. Routine bend-test facilities are used to measure the strengths of the Vickers-indented test pieces. The resulting indentation/strength data are then analyzed in terms of the theoretically predicted fracture toughness equations, and are used to obtain an appropriate "calibration" factor for ceramics. In this context, an earlier preference for the Knoop system as the means for indentation precracking,⁷ on the grounds that it produces a relatively simple fracture geometry, would appear to have no particular justification here.

II. Background Theory

Consider the Vickers-induced radial crack system, characteristic dimension c , subjected to an applied tensile stress σ_a , as depicted in Fig. 1. If the applied loading is uniaxial the indentation is aligned with one set of pyramidal edges parallel to the tensile axis, if biaxial no such alignment is necessary (note that the lateral cracks experience no loading in either case). The stress intensity factor appropriate to this tensile loading has the standard form¹⁴

$$K_a = \sigma_a (\pi \Omega c)^{1/2} \quad (1)$$

Here Ω is a crack-geometry factor which embraces free-surface effects, ellipticity in the radial/median profile,⁷ and crack-interaction (radial/radial, radial/lateral) terms. Conventional strength theory asserts that (in the absence of any other crack

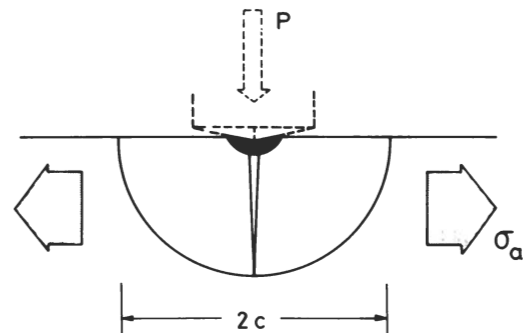


Fig. 1. Schematic of Vickers-produced radial/median crack system, characteristic dimension c , with contributions to tensile loading from applied field at stress σ_a and residual field (via central deformation zone) at (preceding) contact load P .

Received October 22, 1980; revised copy received March 3, 1981.
Supported by the Australian Research Grants Committee, the Australian Department of Defence, and the U. S. Office of Naval Research.
*Member, The American Ceramic Society.
*Now with the Materials and Molecular Research Division, Lawrence Berkeley Laboratory, Berkeley, California 94720.

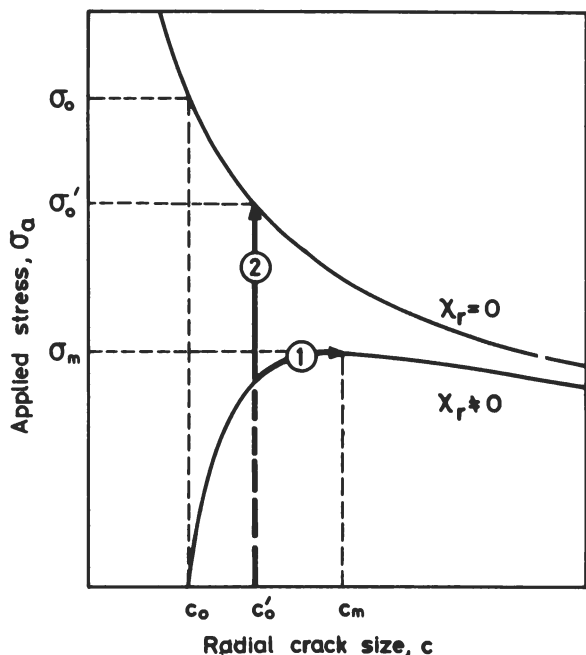


Fig. 2. Plot of function $\sigma_a(c)$ in Eq. (5) for radial cracks with and without residual contact stresses. Note respective strength configurations for crack initially at c'_0 , i.e. activated failure at $\sigma_a = \sigma_m$ via path 1, and spontaneous failure at $\sigma_a = \sigma'_0$ (σ'_0 for special case $c'_0 = c_0$) via path 2. Note also increasing ratio σ_m/σ'_0 as c'_0 increases within range $c_0 \leq c'_0 \leq c_m$.

driving forces) failure will occur spontaneously from the starting flaw at some critical stress level, provided a state of mechanical equilibrium is maintained throughout the tensile loading. Writing the critical conditions as $\sigma_a = \sigma'_0$ at $K_a = K_c$, Eq. (1) gives the strength

$$\sigma'_0 = K_c / (\pi \Omega c'_0)^{1/2} \quad (2)$$

where c'_0 is the size of the radial crack immediately prior to application of the tensile stress (c_0 , if postindentation slow crack growth does not occur); here the stress notation serves to emphasize that, in the absence of any residual contact field, the strength is a function of the initial crack configuration.

However, for the radial crack system of Fig. 1 the term in Eq. (1) is not the only driving force acting during the tensile loading. There is also the residual term (Eqs. (2) and (3), Part I⁸), which scales with the peak contact load P ,

$$K_r = \chi_r P / c^{3/2} = \xi_V^R (E/H)^{1/2} P / c^{3/2} \quad (3)$$

where ξ_V^R is a constant for Vickers-produced radial cracks and E/H is the modulus-to-hardness ratio.⁸ The net stress intensity factor is therefore

$$K = K_r + K_a = \chi_r P / c^{3/2} + \sigma_a (\pi \Omega c)^{1/2} \quad (c > c'_0) \quad (4)$$

For growth under equilibrium conditions, $K = K_c$, Eq. (4) may be solved for the applied stress as a function of crack size,

$$\sigma_a = [K_c / (\pi \Omega c)^{1/2}] [1 - \chi_r P / K_c c^{3/2}] \quad (5)$$

Investigation of the extremum requirement $d\sigma_a/dc = 0$ shows that this function has a maximum at

$$\sigma_m = 3K_c / 4(\pi \Omega c_m)^{1/2} \quad (6a)$$

$$c_m = (4\chi_r P / K_c)^{2/3} \quad (6b)$$

According to this description, the indentation crack undergoes a stage of precursor stable growth, from c'_0 to c_m , in attaining an instability configuration at $\sigma_a = \sigma_m$, which now defines the as-indentation strength.¹² It is noted that the strength no longer depends on the value of c'_0 , for all $c'_0 < c_m$.

It is useful to compare the predicted strength behavior for indentation flaws with and without residual stresses via the construction in Fig. 2. Accordingly, the two solid curves are plots of Eq. (5) for nonzero and zero χ_r . For a starting crack in the size range $c_0 < c'_0 < c_m$ the respective strengths, σ_m and σ'_0 , are achieved via paths 1 and 2. Noting from Eq. (4) in Part I⁸ that $c_0 = (\chi_r P / K_c)^{2/3}$, so that, in conjunction with Eq. (6b), $c_m/c_0 = 2.52$, Eqs. (2) and (6a) give the strength ratio

$$\sigma_m/\sigma'_0 = 0.75(c'_0/c_m)^{1/2} = 0.47(c'_0/c_0)^{1/2} \quad (7)$$

Thus the presence of the residual field may reduce the strength by more than a factor of two, depending on the extent of post-indentation growth $c_0 \rightarrow c'_0$.

An expression for the toughness may now be derived from Eq. (6), making use of the definition of χ_r in Eq. (3),

$$K_c = \eta_V^R (E/H)^{1/8} (\sigma P^{1/3})^{3/4} \quad (8)$$

where $\eta_V^R = [(256/27)(\pi \Omega)^{3/2} \xi_V^R]^{1/4}$ is another geometrical constant; at this point the subscript m is dropped from the notation, on the understanding that σ now refers to the as-indentation strength. Thus with the residual-stress term incorporated into the analysis, K_c may be determined from the two readily measurable quantities σ and P , once the remaining parameters in Eq. (8) are known. Again, it is emphasized that no crack measurements are required, although it may be necessary to examine the fractured test piece to confirm that failure has indeed occurred at the indentation flaw (especially at lower contact loads, where prepresent flaws may dominate).

A major consequence of the flaw-size independence of Eq. (8) is an insensitivity to postindentation slow crack growth: neither c_0 nor c'_0 appears in the expression, since it is the growth to c_m which determines the strength. Of course, slow growth effects can be an important factor in the strength test itself¹⁵; however, precautions can be taken in the test procedure to ensure that failure occurs under conditions close to mechanical equilibrium.

As in Part I,⁸ geometrical variations in the indentation pattern can be expected to introduce some secondary complications, which would reflect largely as departures from invariance in η_V^R . Interaction effects between the different crack components (e.g. radial/lateral), and between crack and microstructure (including anisotropy and inhomogeneity factors), need some attention in this regard. However, as mentioned in Section I, since the indentation crack system is likely to be a reasonable facsimile of a typical surface flaw in ceramics, the "effective" toughness evaluated from Eq. (8) is always likely to remain a useful parameter for strength characterization. If it can be established that the radial crack pattern is in fact well-defined, free of such geometrical modifications, the evaluated K_c may then be identified with the true material toughness.

III. Experimental

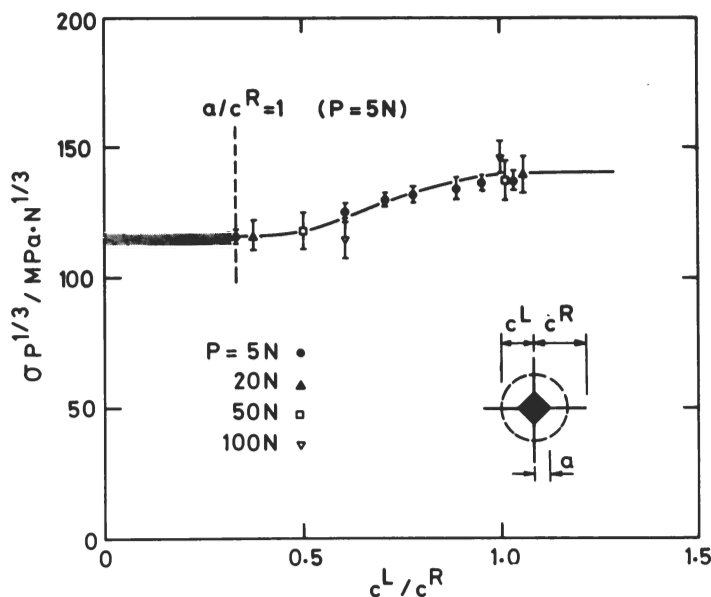
(1) Procedure

Indentation/strength tests were run on the materials listed previously in Table I, Part I.^{8,†} The specimens were prepared in forms suitable for bend testing: soda-lime glass, silicon, and the Coors aluminas as disks, sapphire as rods, and the remainder as bars. In the case of glass and sapphire the test surfaces were mirror smooth; for all other materials the surfaces had a machined finish. It was not considered necessary to produce a high-quality surface finish as in Part I, since no crack measurements are necessary and the presence of preexisting abrasion damage has previously been shown¹⁶ to have little influence on the radial crack response in glass under flexural loading.[‡] A Vickers indentation was made at the center of the prospective tensile face of each test piece, taking care to align the pyramidal edges with respect to the longitudinal axis for the bar and rod specimens. By placing a drop of immersion oil on the

[†] Because of the limited supply of the silicate glass specimens, only the commercially available soda-lime material was included in this part of the study.

[‡] However, in work completed since submission of the present paper (Ref. 17), severe machining damage was demonstrated to have a significant influence on strength properties of ceramics by virtue of an associated residual compressive stress in the damaged surface layer.

Fig. 3. Plot of indentation/strength parameter $\sigma P^{1/3}$ as function of lateral/radial crack-size ratio, c^L/c^R for glass disks indented and broken in oil environment; ratio c^L/c^R is adjusted by varying interval between contact and flexure. (Shaded band at $c^L < a$ for $p = 5$ N indentation designates region where cracks are obscured by deformation zone.) In this work the "saturation" limit $c^L/c^R \rightarrow 1$ is taken as the "standard" Vickers crack configuration (after Ref. 15).



preselected contact site prior to indentation, the access of moisture to the tip regions of the ensuing radial cracks was minimized (but not completely eliminated (see Part I)), thus producing most favorable environmental conditions for approaching the requisite state of mechanical equilibrium in the subsequent strength test. The range of indentation loads covered for each material was limited at the lower end by the size of preexisting flaws, and at the upper end either by the thickness of the available specimens (crack dimensions at failure less than one-tenth specimen thickness) or the incidence of lateral-induced chipping. The bend tests themselves were conducted in conventional ring-on-ring (disks) or four-point support (bars and rods) configurations, with appropriate plate or beam elasticity formulas used to evaluate the failure stresses. A stressing rate of $\approx 10 \text{ MPa} \cdot \text{s}^{-1}$ was chosen, a level at which the effects of slow crack growth in oil environments have been established as negligible.¹⁵

(2) Exploratory Tests

Some exploratory tests were again made on soda-lime glass to investigate certain points of issue arising from the theory. First, the influence of postindentation slow crack growth on the as-indentation strength was examined. This was done by systematically varying the interval between the contact- and bend-test stages, thereby allowing for control of c'_0 as per Fig. 2, Part I.⁸ Rather than remain invariant, as predicted by theory, the strength actually showed a slight tendency to increase with c'_0 . This apparently anomalous behavior could be associated with the relatively sluggish development of the lateral cracks with respect to the radials in the oil environment.⁸ Figure 3 appropriately shows the indentation/strength composite term pertinent to Eq. (8) as a function of experimentally measured lateral/radial crack size.¹⁵ Physically, the result in this plot may be regarded as a measure of residual-stress relief afforded by a compliant lateral system (suggesting that χ_r in Eq. (3) should strictly be replaced by χ'_r , where $\chi'_r < \chi_r$ ¹⁸). Here the "saturation limit," $c^L/c^R \rightarrow 1$, achieved typically within 1 h of the contact, was taken as a standard configuration for the tests proper.

Next, a series of tests was made to confirm the predicted magnitude of the residual-stress effect in the strength characteristics. The surface-removal procedure used by Petrovic *et al.*^{7,9} for silicon nitride and silicon carbide specimens was adapted for this purpose. Soda-lime glass and AD999-grade⁵ alumina, two materials whose crack response was particularly amenable to fractographic analysis,⁸ were selected for study. Silicon carbide grit, 320 mesh for glass and 150 mesh for alumina, was used to grind away the indented surfaces to a given depth prior to strength testing. In these

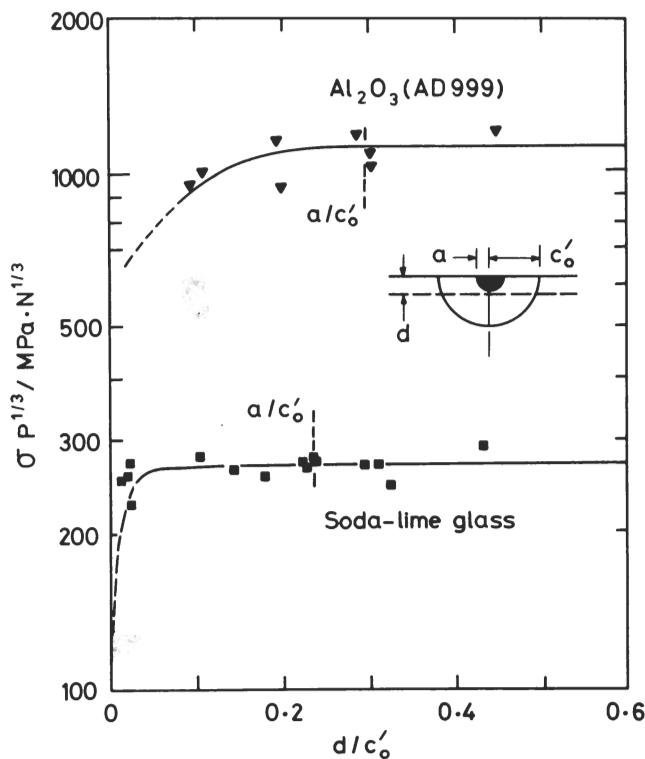


Fig. 4. Plot of indentation/strength parameter $\sigma P^{1/3}$ as function of normalized depth, d/c'_0 , removed by surface abrasion treatment, for glass ($P = 50$ N) and alumina ($P = 100$ N) specimens. Data points are "corrected" strengths (Appendix) for cracks without residual stress, shaded bands "as-indentation" strengths. Scale of deformation zone is indicated for each material.

tests the drop of immersion oil was not placed over the indentation site until completion of the grinding process, and then only after thorough cleaning and drying of the ground surface. Figure 4 shows the results as a function of depth d removed, here normalized to the preabrasion crack parameter c'_0 . Ideally, the removal process should be one which eliminates the source of residual stress without interfering with the crack geometry. However, as seen from the magnitudes of the hardness impression dimensions a indicated in Fig. 4, a substantial portion of the crack is removed before the central deformation zone can be considered nullified.

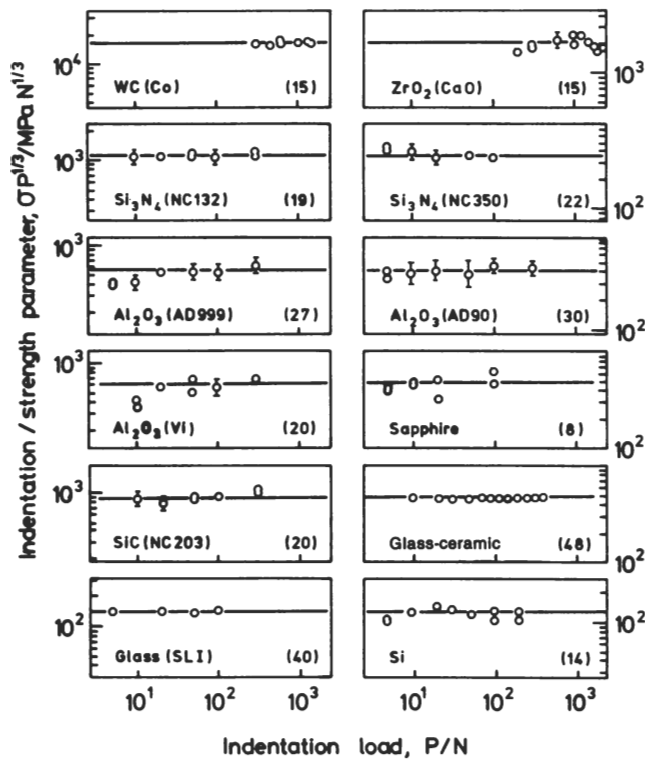


Fig. 5. Plot of $\sigma P^{1/3}$ over working range of load P for each test material. Number of specimens used to determine mean parameter is indicated in each case.

The data points accordingly contain a correction factor in the strength to compensate for the changes in size and shape of the radial/median crack system. A factor is also incorporated to convert the measured strengths to equivalent values for zero post-indentation slow crack growth, i.e. $\sigma'_0 \rightarrow \sigma_0$ in Fig. 2. Details of these two factors are given in the Appendix. Thus the plateau regions of the curves in Fig. 4 correspond to equilibrium indentation/strength characteristics for flaws without residual stress. To be compared with these values are those obtained from as-indenting strength data at maximum residual stress (i.e. at $c^L/c^R=0$; see Fig. 3 for glass), plotted in the figure as the horizontal shaded bands. The predicted strength ratio of 0.47 for $c'_0=c_0$ in Eq. (7) is closely approached for the two materials. It is concluded that the residual-stress theory of strength outlined in Section II is soundly based.

IV. Results

With due attention to the potential complications discussed in the previous section, as-indenting strengths were measured for each material over a range of contact loads. The test pieces were examined before and after failure, for two reasons: (i) to ensure that failure occurred from the indentation site (those that did not were rejected from the data); (ii) to establish whether or not the crack patterns were well defined (see Part I). The results are plotted in Fig. 5, in accordance with Eq. (8). The error bars in this plot are standard deviations for a minimum of five specimens at each contact load (in some cases, notably in glass and glass-ceramic,¹ the error bars are too small to show on the plot), and the fitted lines are the mean values of $\sigma P^{1/3}$ computed over all specimens for each of the materials. It is seen that, within the experimental scatter, $\sigma P^{1/3}$ is reasonably constant over the range of P studied.

Following the procedure in Part I, confirmation of the usefulness of Eq. (8) as a basis for toughness evaluation is established by reconciling the data in Fig. 5 with the material parameters given in Table I.⁸ First, by averaging over the results for the designated "reference" ceramics, a "calibration" constant

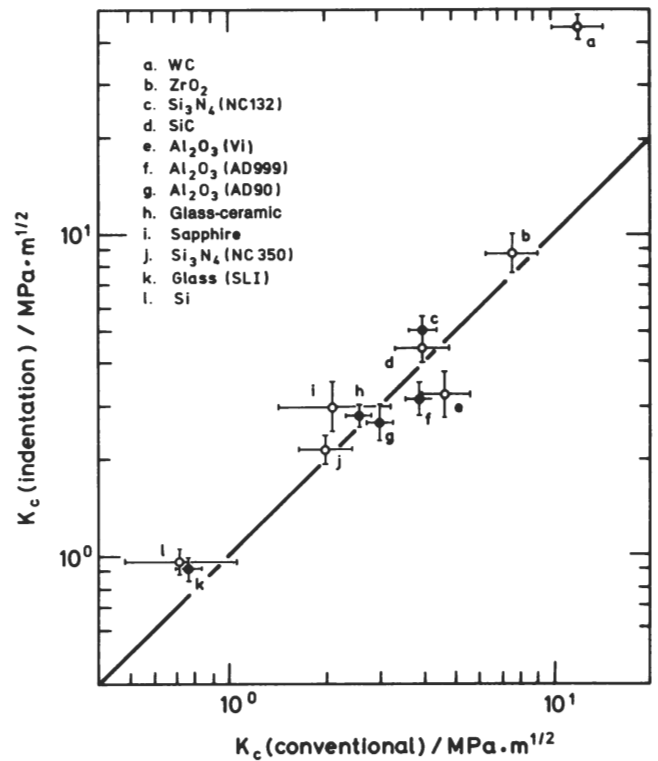


Fig. 6. Plot demonstrating correlation between toughness values determined by indentation and those determined by conventional means. Filled symbols denote reference materials used to evaluate η_V^R in Eq. (8). Vertical error bars represent uncertainty (standard deviation) in parameter $\sigma P^{1/3}$ obtained from Fig. 5, horizontal error bars represent nominal accuracy of K_c values taken from Table I in Part I.

$\eta_V^R = K_c(H/E)^{1/8} / (\sigma P^{1/3})^{3/4} = 0.59 \pm 0.12$ is obtained. With this evaluation, Eq. (8) is then used to compute the toughness for each of the materials represented in Fig. 5. The indentation-determined K_c values thus computed may be compared with the corresponding values determined by conventional means, as in Fig. 6. The degree of fit between the calibrated curve and the individual data points is comparable to that obtained for the analogous plot, Fig. 5, in Part I.

V. Discussion

The plot of Fig. 6, in conjunction with Eq. (8), forms the basis of an alternative indentation technique for evaluating fracture toughness. From the errors in the plotted data, it is estimated that it should be possible to determine K_c for any well-behaved material to within 30 to 40%, i.e. with an accuracy comparable to that indicated for the direct crack measurement technique described in Part I.⁸ In this context, uncertainties in the value of E/H are relatively unimportant; indeed, since this ratio varies only between 10 and 50 for most ceramics, replacement of $\eta_V^R(E/H)^{1/8}$ by an averaged quantity $\eta_V^R = 0.59 < (E/H)^{1/8} > = 0.88$ would add no more than 10% to the error in the K_c evaluation for a material whose elastic/plastic parameters are totally unknown.

On a comparative assessment of advantages and disadvantages, the indentation/strength technique has certain points of appeal. Foremost among these is the fact that no crack measurements need be made; crack size is eliminated as a test variable in favor of indentation load, which is much more easily monitored. Also, by virtue of the "energy barrier" to failure associated with the presence of the residual contact stresses, the results are relatively insensitive to postindentation slow crack growth phenomena. It is nevertheless considered important to establish that the radial crack evolution in any given test material is well behaved before identifying K_c evaluated from Eq. (8) with the true toughness. For those cases with

ill-defined crack patterns, namely the Vi-grade *Al_2O_3 , ZrO_2 , and WC, the effective K_c evaluated may no longer reflect macroscopic crack behavior, although it may remain a useful parameter for characterizing the response of the typical surface flaw. For instance, the indentation/strength approach would be most appropriate for predicting the strength degradation characteristics in ceramic surfaces subjected to incidental sharp-particle contact events, notably under impact conditions, where the dominant flaws are expected to possess all the essential features of the radial/median system used as the basis of the present studies.^{16,19,20} On the debit side, the indentation/strength technique lacks the economy of its direct crack measurement counterpart, producing only one result per specimen, although this is balanced somewhat by the less stringent surface preparation requirements. Again, it is necessary to ensure that the specimens contain no built-in stresses prior to indentation⁸; violation of this condition should be readily apparent by departures from constancy of the quantity $\sigma P^{1/3}$ in the plots of Fig. 5.^{20,21}

Thus, by incorporating a residual contact stress term into the analysis of brittle failure we have been able to devise an alternative indentation method for determining the toughness of ceramics, one which at the same time overcomes previous objections⁷ and introduces certain unique advantages in the test procedure. With its foundations deeply rooted in the theory of strength, the method offers some insight into the concept of fracture toughness at the level of the microscopic flaw.

APPENDIX

CORRECTION FACTORS FOR STRENGTH OF SURFACE-GROUND SPECIMENS WITH INDENTATION CRACKS

As noted in Section III, a meaningful comparison of strengths for indented specimens with and without residual contact stresses may require the incorporation of geometrical correction factors into the analysis. Such factors are considered here, in particular relation to the surface-removal technique used to obtain the data points in Fig. 4.

Consider the radial/median crack geometry in Fig. A1. In line with observations made in Part I⁸ and elsewhere⁷ the profile is taken to be elliptical, initially with semimajor surface axis c_0' and semiminor depth axis b_0' . After removal of a surface layer to depth d , the respective axes become (with the remnant segment still assumed elliptical) c_0'' and b_0'' , connected to the initial dimensions via the transformation relations

$$c_0'' = c_0' (1 - d^2/b_0'^2)^{1/2} \quad (A-1a)$$

$$b_0'' = b_0' (1 - d/b_0') \quad (A-1b)$$

These equations may be used to convert strengths measured after surface removal to equivalent values at $d=0$. The general expression for the strength appropriate to an elliptical crack of semiaxes c and b , free of any residual stresses, may be written

$$\sigma = K_c \Phi(b/c) / m (\pi b)^{1/2} \quad (A-2)$$

where m is a configuration term which incorporates effects of the specimen free surface, mutually orthogonal radial/median cracks, etc., and the function $\Phi(b/c)$ is the elliptic integral

$$\Phi(b/c) = \int_0^{\pi/2} [\cos^2 \psi + (b/c)^2 \sin^2 \psi]^{1/2} d\psi \quad (A-3)$$

with ψ a dummy variable. Equation (A-2) is of the same form as our Eq. (2), where we identify $\Omega(b/c) = [\Phi(b/c)/m]^2$. Now putting $\sigma = \sigma_0'$ at $c = c_0'$ and $b = b_0'$ for the strength before surface removal, and likewise $\sigma = \sigma_0''$ at $c = c_0''$ and $b = b_0''$ for the strength after removal, Eq. (A-2) gives

$$\sigma_0' = \sigma_0'' \{ (b_0''/b_0')^{1/2} [\Phi(b_0'/c_0') / \Phi(b_0''/c_0'')] \} \quad (A-4)$$

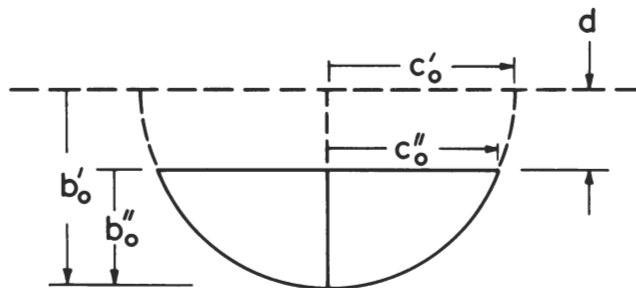


Fig. A1. Dimensions of radial/median crack subject to surface removal to depth d .

Next, consider the effect that postindentation slow crack growth $c_0 \rightarrow c_0'$ has on the strength. From Eq. (2) it is seen immediately that

$$\sigma_0 = \sigma_0' (c_0'/c_0)^{1/2} \quad (A-5)$$

Thus Eqs. (A-4) and (A-5) may be used to convert the strengths σ_0'' measured on surface-ground specimens to the equivalent values σ_0 that would have obtained had no crack area been removed and no postindentation slow crack growth occurred:

$$\sigma_0 = \sigma_0'' \{ [(c_0'/c_0)(b_0''/b_0')]^{1/2} [\Phi(b_0'/c_0') / \Phi(b_0''/c_0'')] \} \quad (A-6)$$

It follows from the transformation relations in Eq. (A-1) that the composite conversion factor within the braces is a unique function of c_0'/c_0 and b_0''/b_0' for any specified value of the initial ellipticity factor b_0'/c_0' . Evaluation of this equation as a function of surface-removal parameter d/c_0' then involves measurement of the initial ellipticity factor b_0'/c_0' from the section fractography and c_0'/c_0 from Fig. 3 of Part I.⁸

References

- R. K. Govila, "Cleavage Fracture of VC Monocrystals," *Acta Met.*, **20** [3] 447-57 (1972).
- J. J. Petrovic and L. A. Jacobson; pp. 397-414 in *Ceramics for High Performance Applications*. Edited by J. J. Burke, A. E. Gorum, and R. N. Katz. Brook Hill, Chestnut Hill, Mass., 1974.
- N. Ingelstrom and N. Nordberg, "The Fracture Toughness of Cemented Tungsten Carbides," *Eng. Fract. Mech.*, **6** [3] 597-607 (1974).
- J. J. Petrovic, L. A. Jacobson, P. K. Talty, and A. K. Vasudevan, "Controlled Surface Flaws in Hot-Pressed Si_3N_4 ," *J. Am. Ceram. Soc.*, **58** [3-4] 113-66 (1975).
- R. R. Wills, M. G. Mendiratta, and J. J. Petrovic, "Controlled Surface Flaw-Initiated Fracture in Reaction-Bonded Si_3N_4 ," *J. Mater. Sci.*, **11** [7] 1330-34 (1976).
- J. J. Petrovic and L. A. Jacobson, "Controlled Surface Flaws in Hot-Pressed SiC," *J. Am. Ceram. Soc.*, **59** [1-2] 34-37 (1976).
- J. J. Petrovic and M. G. Mendiratta; pp. 83-102 in *Fracture Mechanics Applied to Brittle Materials*. Edited by S. W. Freiman. *ASTM Spec. Tech. Publ.*, No. 678, Philadelphia, 1979.
- G. R. Anstis, P. Chantikul, B. R. Lawn, and D. B. Marshall, "A Critical Evaluation of Indentation Techniques for Measuring Fracture Toughness: I"; this issue pp. 533-38.
- J. J. Petrovic, R. A. Dirks, L. A. Jacobson, and M. G. Mendiratta, "Effects of Residual Stresses on Fracture from Controlled Surface Flaws," *J. Am. Ceram. Soc.*, **59** [3-4] 177-78 (1976).
- M. V. Swain, "A Note on the Residual Stress About a Pointed Indentation Impression in a Brittle Solid," *J. Mater. Sci.*, **11** [12] 2345-48 (1976).
- D. B. Marshall and B. R. Lawn, "Residual Stress Effects in Sharp Contact Cracking: I," *ibid.*, **14** [8] 2001-12 (1979).
- D. B. Marshall, B. R. Lawn, and P. Chantikul, "Residual Stress Effects in Sharp Contact Cracking: II," *ibid.*, [9] 2225-35.
- B. R. Lawn, A. G. Evans, and D. B. Marshall, "Elastic/Plastic Indentation Damage in Ceramics: The Median/Radial Crack System," *J. Am. Ceram. Soc.*, **63** [9-10] 574-81 (1980).
- B. R. Lawn and T. R. Wilshaw, *Fracture of Brittle Solids*; Ch. 3. Cambridge University Press, London, 1975.
- D. B. Marshall and B. R. Lawn, "Flaw Characteristics in Dynamic Fatigue The Influence of Residual Contact Stresses," *J. Am. Ceram. Soc.*, **63** [9-10] 532-36 (1980).
- B. R. Lawn, E. R. Fuller, and S. M. Wiederhorn, "Strength Degradation of Brittle Surfaces: Sharp Indenters," *ibid.*, **59** [5-6] 193-97 (1976).
- R. F. Cook, B. R. Lawn, T. P. Dabbs, and P. Chantikul, "Effect of Machining Damage on the Strength of a Glass-Ceramic"; this issue, pp. C-121-C-122.
- B. R. Lawn, D. B. Marshall, and P. Chantikul, "Mechanics of Strength-Degrading Contact Flaws in Silicon"; unpublished work.
- S. M. Wiederhorn and B. R. Lawn, "Strength Degradation of Glass Impacted with Sharp Particles: I," *J. Am. Ceram. Soc.*, **62** [1-2] 66-70 (1979).
- B. R. Lawn, D. B. Marshall, P. Chantikul, and G. R. Anstis, "Indentation Fracture: Applications in the Strength of Ceramics," *J. Aust. Ceram. Soc.* **16** [1] 4-9 (1980).
- D. B. Marshall and B. R. Lawn, "Strength Degradation of Thermally Tempered Glass Plates," *J. Am. Ceram. Soc.*, **61** [1-2] 21-27 (1978).